Chapter 3

Unidirectionally, Laterally Loaded Dowel-Type Fasteners Multiple-Bolt Joints

3.1 General

For many years U.S. design codes modeled the design values of a multiple-bolt joint as the design value of a single-bolt connection multiplied by the number of bolts. The provisions were based on research conducted by Trayer (1932) who observed an equal distribution of load among bolts. This was despite the fact that research conducted as early as in the late 19th century suggested an uneven load distribution among fasteners of metal joints. Today however, it is widely agreed that the strength of a multiple-bolt timber connection loaded statically in one direction is less than *n* times the capacity of a single-bolt joint, where *n* stands for the number of bolts. That is, the individual bolts in a multiple-bolt joint do not share the applied load equally, resulting in higher stressed fasteners at certain locations. Individual fasteners fail before other fasteners in the same row are able to carry their maximum load. Hence, for stiff fasteners such as bolts, the total strength of a multiple-bolt joint loaded one-directionally must be smaller than the sum of the capacities of the individual fasteners.

To assure safe design, the concept of *effective number of fasteners* was introduced (Fahlbusch 1949; Lantos 1969; Jorissen 1998).

$$Z_{multiple} = n_{effective} \cdot Z_{\text{single}} \cdot K \tag{3.1}$$

		Unit
Z	lateral design load	N
$n_{effective}$	effective number of fasteners in a row (< actual number of fasteners)	
K	safety factor	

3.2 Key Parameters Influencing Multiple-bolt Joint Behavior

All parameters that influence single-bolt joints affect the performance of multiple-bolt joints as well. Furthermore, multiple-bolt connection behavior is sensitive to variables such as

modulus of elasticity of the members, fastener aspect ratio, material discontinuities, and loading direction. Multiple-bolt connection behavior is, however, thought most sensitive to parameters including fabrication tolerances, the number of bolts in a row or column, and the arrangement of the individual fasteners (i.e. spacing, number of rows, etc.).

3.2.1 Fabrication Tolerances

Fabrication tolerances can have two possible effects (Moss 1996). One effect is that oversized holes result in random distribution of initial slip at near zero loads. The other effect is slippage at low loads due to slight misalignment of the bolt holes with direction of loading.

According to Wilkinson (1986), due in part to misdrilled holes, any particular row of bolts has a unique load distribution. Bolts randomly start sharing the joint load at increasing slip depending on initial alignment of bolt and hole resulting in a variable joint slip modulus for the entire connection (Salenikovich et al. 1996). This implies that $n_{effective}$ as defined in Section 3.1 changes as the applied load on the entire joint increases. Salenikovich et al. (1996) found through tests of 6 bolts (19 mm diameter) in a row that $n_{effective}$ increased from approximately 0.18 to 0.9 with increasing load up to capacity. In addition, the work stated that the influence of oversized holes diminished at loads close to capacity and that the load distribution approached that predicted by linear elastic models. Lantos (1968) observed that the effect of manufacturing tolerances might be less with increasing number of rows of bolts per connection.

3.2.2 Fastener Aspect Ratio

Multiple fastener joints containing fasteners with high aspect ratios (i.e. slender) tend to fail in bearing rather than premature splitting. If tight fit is assumed, load distribution among the fasteners is then primarily affected by the load-slip characteristics of the individual fasteners, which in turn are a function of varying local material properties. Fastener aspect ratio is directly correlated with fastener stiffness. Fastener stiffness, relative to joint stiffness, significantly affects load distribution among fasteners. According to linear elastic analysis, the stiffer the bolts relative to the members (i.e. bolts with small aspect ratios) the greater are load concentrations among fasteners.

3.3 Mathematical Models

The behavior of multiple-bolt joints is still not fully understood due to the interactions of complex stress distributions, manufacturing tolerances and material discontinuities. A number of mathematical models have been suggested in the literature for multiple fastened joints loaded

parallel to the grain. Very little, if any, analytical research has been conducted regarding multiple bolts loaded perpendicular to the grain, not least because large stresses perpendicular to the grain are introduced, which greatly limit applicability. The following section reviews major analytical formulations that have been published in the past and that form the foundation of the solution derived in this work.

3.3.1 Linear Elastic Formulations

According to linear elastic models devised in the past (Cramer 1968, Lantos 1969, Wilkinson 1986), the force distribution in main and side members changes in a stepwise function from fastener to fastener and remains constant between fasteners. The fastener is assumed to be the sole means of load transfer from the main member to the two side members (Figure 3.1). Note that the stepwise decreases or increases in force are not equal. The shape of the discrete steps depends on number of fasteners in a row, modulus of elasticity of the joint members, fastener load-slip characteristic, and spacing between individual bolts. Due to a change in member force caused by transfer through the bolts, stresses and consequently strains of the members change from section to section. Within any one section, side and main member strains are not equal. The difference is compensated for by bolt deformation. Assuming tight fit, maximum load is reached first in the bolt at the beginning or the end of the fastener row because the stress and associated elongation is greatest in the main member when it is near zero in the side members.

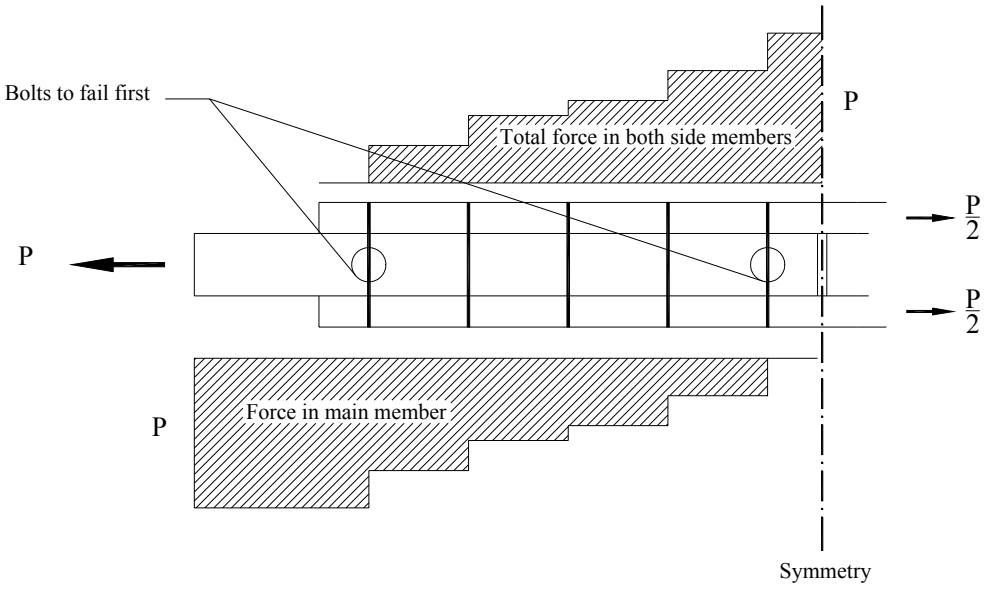

Figure 3.1: Load distribution according to linear elastic theory

Figure 3.2 depicts the basic displacement compatibility between the fasteners and members of a joint in single shear. Expressed mathematically and assuming linear elastic behavior of the members, the displacement relationship can be written as

$$\Delta_i + a + u_1 = \Delta_{i+1} + a + u_2 \tag{3.2}$$

where,

$$u_1 = \frac{P_{m1;i} \cdot a}{E_1 \cdot A_1} \tag{3.3}$$

$$u_2 = \frac{P_{m2;i+1} \cdot a}{E_2 \cdot A_2} \tag{3.4}$$

$$\Delta_i = \frac{F_i}{K} \tag{3.5}$$

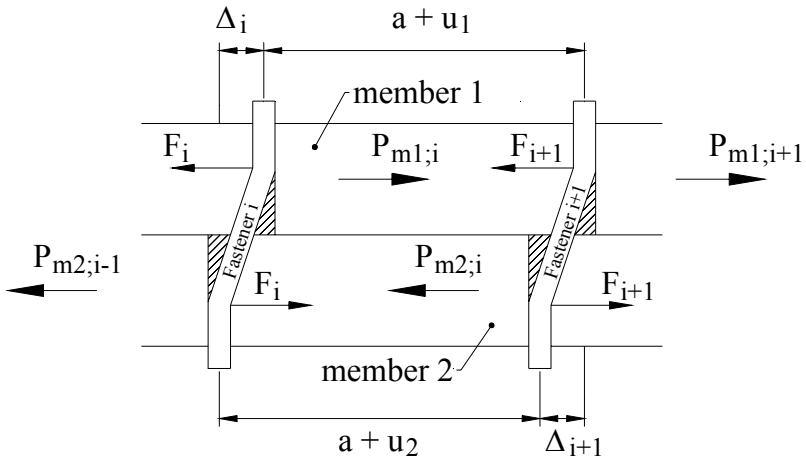

Figure 3.2: Displacement compatibility relationship (balancing moments are not shown).

		Unit
Δ_i	displacement of fastener *i*	mm
a	spacing between fasteners	mm
d	fastener diameter	mm
u_1, u_{2x}	extension of member 1 and 2, respectively	mm
E_1, E_2	modulus of elasticity of member 1 or 2, respectively	N/mm^2
$P_{m1;i}$	load between two fasteners of member 1	N
F_i	load at fastener *i*	N
K	slip modulus describing load slip relationship of fasteners	N/mm

Models described in the literature mainly differ in the determination of the slip modulus *K* (load deflection characteristic of the fasteners) but make use of the same initial approach as outlined above. In the US, Lantos (1969) and Cramer (1968) independently developed a solution for a tension joint in double shear. Both formulations are based on the assumptions that fastener load stays within the elastic range and that there is no clearance between bolt and hole. Lantos took a design-oriented approach and derived solutions only for the two bolts at critical locations. The load deflection characteristic of the individual bolt was simply modeled as linearly elastic (Figure 3.3) and expressed in terms of the "joint slip modulus" γ, which was assumed to be equal and constant for each bolt in the connection.

$$K = \frac{P_f \cdot \text{permissible}}{\Delta} \tag{3.6}$$

		Unit
K	joint slip modulus	N/m
P_f	lateral load carried by fastener	N
Δ	joint slip at permissible load	m

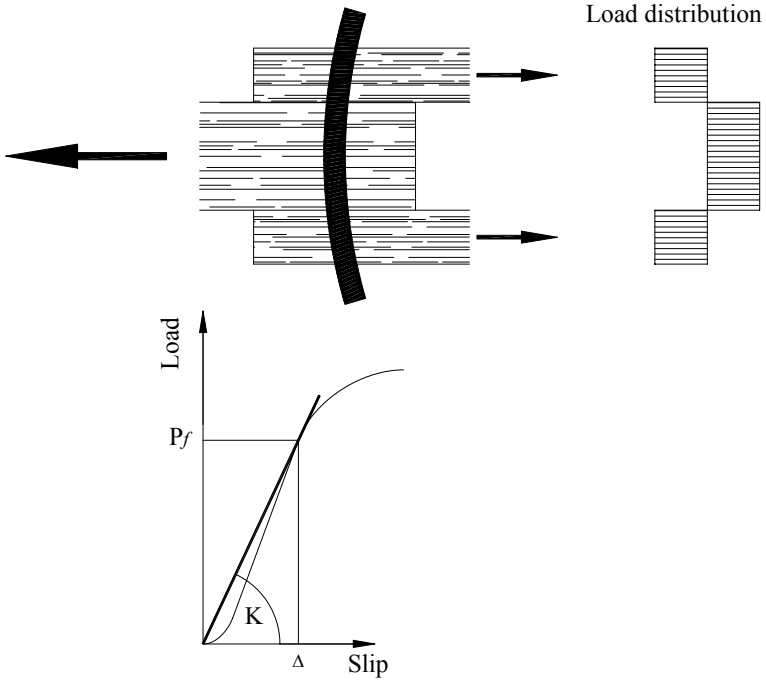

Figure 3.3: Assumed fastener behavior by Lantos (1969).

If the first and last bolt in the row is not to exceed the maximum allowable lateral load, the effective number of fasteners is determined as follows

$$n_{effective} = \frac{1}{C_1} \quad [\text{for } C_1 > C_2]$$
$$n_{effective} = \frac{1}{C_2} \quad [\text{for } C_2 > C_1] \tag{3.7}$$

where,

$$C_1 = 1 - \xi_1 \cdot (1+\mu) + \mu + (\xi_1 - \xi_2) \cdot \frac{\xi_1^n \cdot (1+\mu) - \mu}{\xi_1^n - \xi_2^n} \tag{3.8}$$

$$C_2 = -\mu + \xi_1^{(n-1)} \cdot (1+\mu) - \left(\xi_1^{(n-1)} - \xi_2^{(n-1)}\right) \cdot \frac{\xi_1^n \cdot (1+\mu) - \mu}{\xi_1^n - \xi_2^n} \tag{3.9}$$

and

$$\mu = -\frac{1}{1 + \dfrac{E_m \cdot A_m}{E_s \cdot A_s}} \tag{3.10}$$

$$\xi_1 = \frac{\omega + \sqrt{\omega^2 - 4}}{2} \tag{3.11}$$

$$\xi_2 = \frac{\omega - \sqrt{\omega^2 - 4}}{2} \tag{3.12}$$

$$\omega = 2 + K \cdot a \cdot \left[\frac{1}{E_m \cdot A_m} + \frac{1}{E_s \mp A_s} \right] \tag{3.13}$$

		Unit
E_m	modulus of elasticity of main member	N/m^2
E_s	modulus of elasticity of side member	N/m^2
A_m	cross sectional area of main member	m^2
A_s	cross sectional area of side member	m^2
a	fastener spacing	m
K	joint slip modulus	N/m

Lantos noted that increased joint stiffness (e.g. through the use of bolts with smaller aspect ratios) leads to greater load concentration. Yet, his solution does not consider failure through premature splitting of the timber, which is often observed in multiple-bolt connections containing rigid fasteners. In order for the model to give acceptable results, the underlying assumption that individual fastenings fail in bearing rather than premature splitting must be met. Lantos did not experimentally validate the model.

Cramer (1968) modeled the individual fastener as a beam on an elastic foundation with a linear correlation between load and overall joint displacement based on work published by Stluka

(1966) to account for non-uniform load distribution along the fastener. Similar to Lantos, Cramer's formulation is derived from a three-member joint but with metal side plates instead of only wood members. Cramer simplified the problem by considering the individual bolt to be supported by a linear elastic foundation (thick main member) and subjected to a concentrated force at each end (thin metal plates) (Figure 3.4). Joint stiffness K is a composite of the elastic wood foundation modulus, k_m, and localized bearing stiffness of bolt and metal side plates, k_s.

$$K = k_s + k_m \tag{3.14}$$

where,

$$k_s = \frac{1}{2 \cdot t_s \cdot E_b} + \frac{1}{2 \cdot t_s \cdot E_p} \tag{3.15}$$

$$k_m = \frac{\lambda}{k_w} \cdot \left(\frac{\cosh(\lambda \cdot t_m) + \cos(\lambda \cdot t_m)}{\sinh(\lambda \cdot t_m) + \sin(\lambda \cdot t_m)} \right) \tag{3.16}$$

and,

$$\lambda = \sqrt[4]{\frac{k_w}{4 \cdot E_b \cdot I_b}} \tag{3.17}$$

$$\frac{1}{k_w} = \frac{1}{2 \cdot \pi \cdot (E_l - E_t)} \left[\frac{\left(\frac{E_t}{E_l} + \nu_{tl} \right)^2}{\frac{E_t}{E_l}} - \frac{(1 + \nu_{tl})^2}{\sqrt{\frac{E_t}{E_l}}} \right] \cdot \ln\left(\frac{d}{2 \cdot a + d} \right) \tag{3.18}$$

		Unit
k	Joint stiffness of individual bolt	N/m
k_s	localized bearing stiffness of bolt and metal side plates	N/m
k_m	bolt deflection factor on wood foundation if loaded as in Figure 3.4	N/m
k_w	wood foundation modulus	N/m
E_b	modulus of elasticity of bolt	N/m^2
E_p	modulus of elasticity of metal side plates	N/m^2
E_l	longitudinal modulus of elasticity of wood	N/m^2
E_t	tangential modulus of elasticity of wood	N/m^2
ν_{tl}	Poisson's ratio of wood between tangential and longitudinal direction	
I_b	moment of inertia of bolt	m^4
a	fastener spacing	m
t_m	thickness of main member	m
t_s	thickness of side member	m
λ	coefficient	

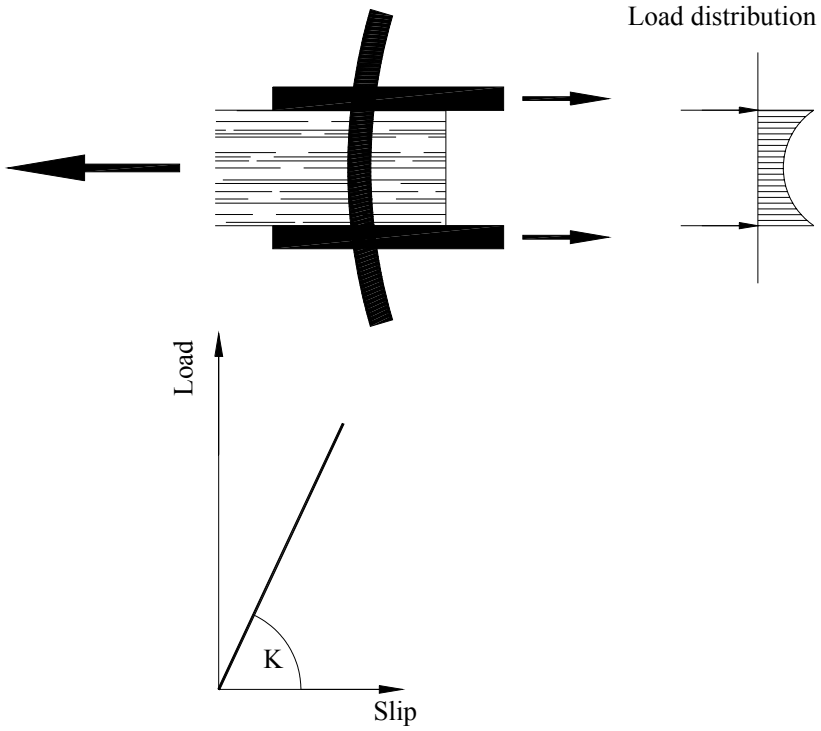

Figure 3.4: Fastener behavior as assumed by Cramer (1968)

As opposed to Lantos, Cramer accounted for the effect of bolt holes on strain. He made use of a stress concentration factor developed by Schulz (1938). Irregularities such as bolt holes result in stress concentrations that cause increased local strains. In general, Cramer's approach is very similar to that of Lantos' but is based on fewer assumptions, as it accounts for stress concentration and non-uniform load distribution effects.

The shortcoming of these models is the exclusion of fabrication tolerances and the assumption of equal and linear load-slip behavior among the fasteners. Cramer verified his model with perfectly machined joints and found that only the slightest misalignment of bolts could cause significant deviation from predicted results due to a changed load distribution among bolts.

Wilkinson (1986) expanded upon Lantos' solution to include fabrication tolerances and to approximate the load slip relation of each bolt by a piecewise linear load-slip curve as shown in Figure 3.5. The model allows for input of a different load-slip relation for each individual bolt, which represents changing material properties. After comparison of analytical models, the researcher concluded that the inclusion of nonuniform stress distribution due to reduced cross section (as done by Cramer) results in insignificantly different results from simpler models.

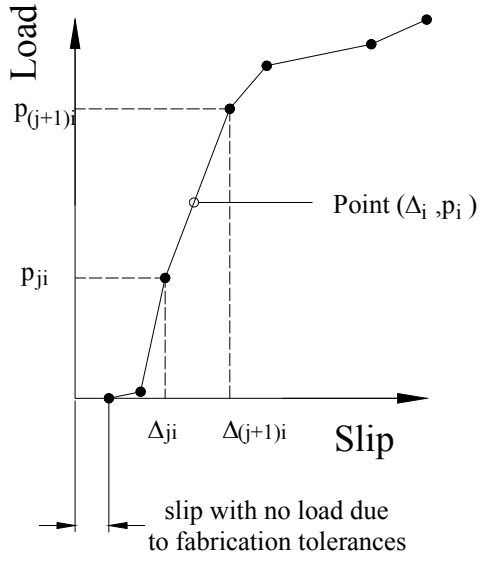

Figure 3.5: Piecewise linear load-slip curve of fastener *i* used by Wilkinson (1986)

According to Figure 3.5 the slope of any line segment for fastener *i* can be described as

$$K_{ji} = \frac{p_{(j+1)i} - p_{ji}}{\Delta_{(j+1)i} - \Delta_{ji}} \tag{3.19}$$

and the deformation of bolt *i* can be expressed in accordance with Equation (3.20).

$$\Delta_i = \Delta_{ji} + K_{ji}^{-1} \cdot \left(p_i - p_{ji}\right) \tag{3.20}$$

		Unit
K_{ji}	slope of straight line segment *j* and fastener *i*	N/mm
p_{ji}	nodal load value of straight line segment *j* and fastener *i*	N
Δ_{ji}	nodal displacement value of straight line segment *j* and fastener *i*	mm

Moss (1996) determined a maximum slippage value due to fabrication tolerances based on requirements by the New Zealand Building Code. He then multiplied this value by a random number in the range of 0 and 1 to randomly assign initial slippage to the individual fastener.

3.3.2 Stochastic Model by Blass

The analytical formulations discussed so far all determined an average load slip response for the individual fasteners, which was assumed to be a single function with no distribution attached. Indeed, the fact that the response obtained actually stems from a distribution of responses was neglected. Blass (1994) used Wilkinson's model and incorporated variation of load-slip performance of the single fasteners. In an effort to simulate the behavior of thousands of joints, Blass employed Foschi's (1974) approximation to determine the capacity of multiple nailed joints in double shear. He fit the curve to the load-slip relationship of single nailed joints in double shear using least squares analysis, although the function describes the load-slip characteristic of a foundation rather than that of the joint as a whole. Blass added the constraint that the load of any single fastener was not to exceed the maximum capacity of a single fastener joint.

$$p(x) = \left(P_0 + P_1 \cdot x\right) \cdot \left(1 - e^{\frac{-k \cdot x}{P_0}}\right) \leq P_{\text{single}} \tag{3.21}$$

		Unit
$p(x)$	fastener lateral load at slip x	N
k	initial stiffness	N/mm
P_{single}	capacity of single fastener joint	N
P_1	slope of the asymptote	N/mm
P_0	y-intercept	N
x	slip	mm

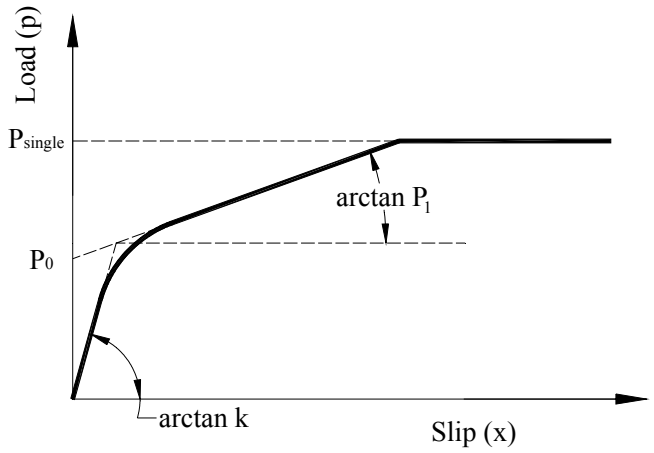

Figure 3.6: Empirical load-slip function used by Blass (1993) based on Foschi (1974)

Curve fitting to a large sample size of tested joint configurations gave information about statistical correlation among function parameters, individual load-slip functions among a row of fasteners, and correlation among individual fasteners arranged in different rows. The result was a three-dimensional correlation matrix. Together with the experimentally determined variances, it was possible to generate random numbers as input parameters with the same variance and covariance structure as actual measured values and simulate the behavior of hundreds of individual fasteners within a joint. Subsequently, maximum load of each simulated joint was calculated using Wilkinson's formulation resulting in a distribution of load values.

With the inclusion of variability, Blass could not find a significant influence of the number of nails in a row on ultimate connection strength for up to 40 nails in a row. This provides additional support to the hypothesis that small diameter fasteners yielding in Mode IV should not exhibit group action behavior.

3.3.3 The Jorissen Model

Jorissen's (1998) model is a hybrid of the elastic formulations developed by Lantos (1969) and stress analysis to include behavior in the inelastic range. Jorissen determined shear stresses and stresses perpendicular to the grain to predict failure due to splitting and to establish an analytical formulation that considers load redistribution due to accumulated stresses around single bolts beyond the elastic range. The mechanical model, as depicted in Figure 3.7, allows for input of different non-linear load slip functions for each individual fastener, but assumes linear elastic deformations of the timber in-between bolts. In line with Lantos' approach, Jorissen computed the load per fastener by

$$\delta_i = \delta_{i-1} + \frac{\sum_{t=1}^{i-1} F_t}{k_{m;i-1}} = \sum_{j=2}^{i} \left(\frac{\sum_{t=j}^{n} F_t}{k_{s;j-1}} \right) + \Delta_i \tag{3.22}$$

where:

$$\Delta_i = \frac{F_i}{k_{f;i}} \tag{3.23}$$

$$k_{s;i} = \frac{E_{s;i} \cdot A_s}{a_i} \tag{3.24}$$

$$k_{m;i} = \frac{E_{m;i} \cdot A_m}{a_i} \tag{3.25}$$

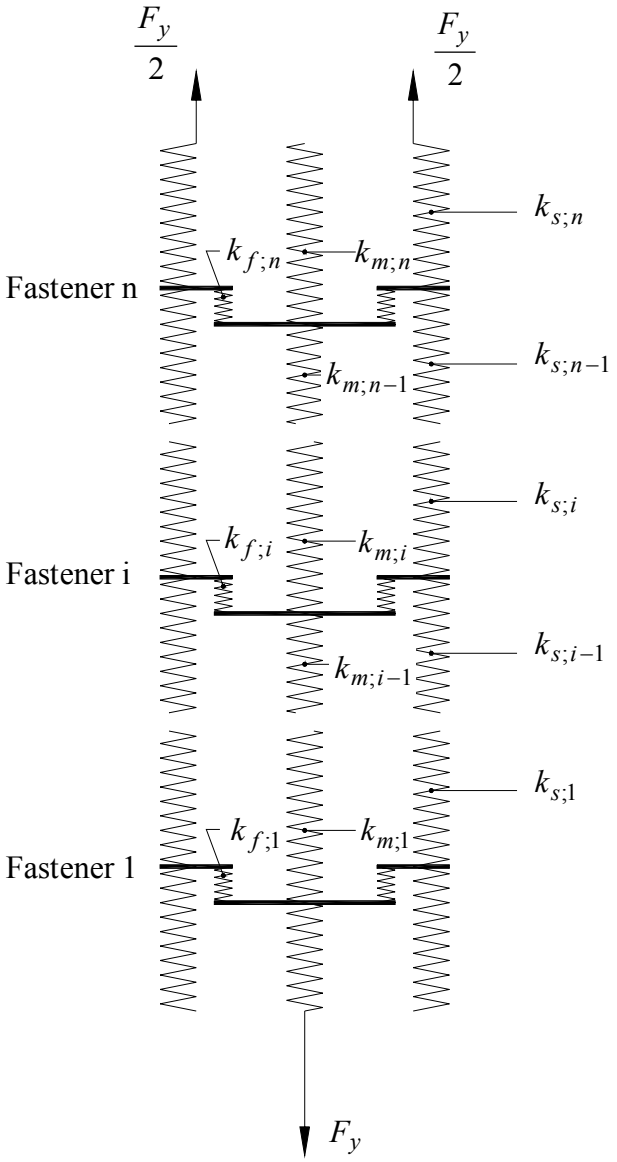

Figure 3.7: Jorissen's mechanical model (after Jorissen, 1998)

To acquire fastener stiffness as a function of lateral load or slip, the individual non-linear load-slip function was obtained using Foschi's (1976) equation as modified by Blass (1994) and shown in Figure 3.6. The curve was shifted in x-direction by a random slack variable, δ_0, resulting in Equation (3.26) to account for oversized holes.

$$F_i(\Delta_i) = \left[P_0 + P_1 \cdot (\Delta_i - \delta_0)\right] \cdot \left(1 - e^{\frac{-k \cdot (\Delta_i - \delta_0)}{P_0}}\right) \leq P_{\text{single}} \tag{3.26}$$

		Unit
$F_i(\Delta_i)$	Lateral load of fastener *i* at slip Δ_i	N
Δ_i	slip of fastener *i*	mm
a_i	spacing between fastener *i* and *i+1*	mm
δ_i	total joint slip at fastener *i* including deformation of timber (see Figure 3.7)	mm
k_f	fastener stiffness as determined from	
k_m, k_s	longitudinal stiffness of main and side members	N/mm
E_m, E_s	modulus of elasticity of main and side members	N/mm^2
A_m, A_s	cross sectional area of main and side members	mm^2
p	reaction force of foundation	N
k	initial stiffness	N/mm
P_{single}	capacity of single fastener joint	N
P_1	slope of the asymptote	N
P_0	y-intercept	N

Forces perpendicular to the grain, due to wedging, effects introduce stresses perpendicular to the grain. Jorissen showed that these stresses accumulate in a multiple fastener joint and may exceed the wood tension strength perpendicular to the grain, even for slender fasteners. Jorissen developed an analytical approach based on beam on elastic foundation theory to compute stresses perpendicular to the grain (Figure 3.8). He assumed a linear elastic wood foundation and approximated the foundation modulus, *k*, as described by Equation (3.27). Jorissen suggested that two cracks form beneath the bolt at the perimeter of the hole at an angle to the load that equals the angle of friction, φ (see Figure 2.9).

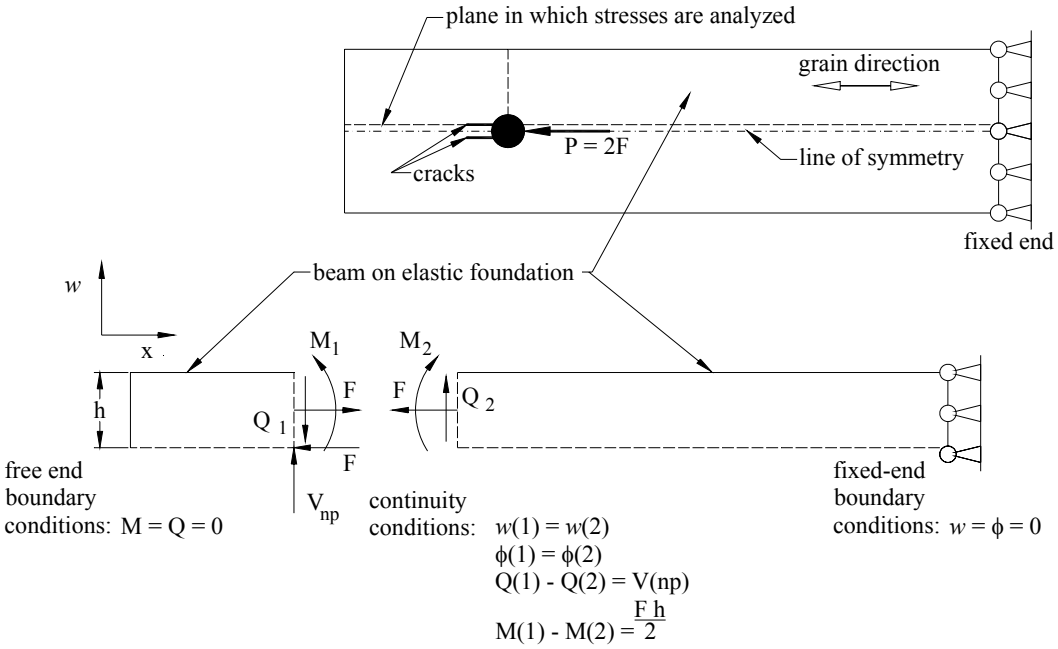

Figure 3.8: Utilization of elastic beam theory to compute stresses perpendicular to the grain (after Jorissen, 1998)

A round bolt may be viewed as a blunt wedge, which explains why forces perpendicular to the grain are introduced when a bolt is laterally loaded in direction parallel to the grain. Derived from a method published by Kuipers (1960), Jorissen calculated the total force perpendicular to the grain (including peak forces). Jorissen found good agreement with numerical results found by Werner (1993).

As depicted in Figure 3.9, peak stresses perpendicular to the grain develop at the crack origins at the fastener hole. Attributed to its macroscopic structure, wood contains small flaws that are equivalent to micro-cracks, which cause a severe concentration of stress perpendicular to the grain at discontinuities such as boltholes. Jorissen assumed that the concentrated stresses perpendicular to the grain at the fastener hole reach the tensile strength of the wood perpendicular to the grain and are the sum of peak stress $\sigma_{p;90}$ and stress due to moment and force perpendicular to the grain (without peak stresses), $\sigma_{np;90}$. The peak stress, σ_p, is found through fracture mechanics analysis. At the tip of a crack, stresses reach the strength of the material and cause intense deformation resulting in an increased area over which the stresses are redistributed (Figure 3.9). The region within which material yielding occurs is frequently called the plastic zone or characteristic crack length (Dowling 1993). Jorissen derived the characteristic crack

length for timber parallel to the grain based on finite element analysis carried out by Gustafsson (1985)). The characteristic length is a function of the critical energy release rate, G_c, which Jorissen determined using the model as suggested by Petersson (1995). The model describes a mixed failure mode resulting from stresses perpendicular to the grain (Mode I) and shear stresses (Mode II) (Figure 3.10).

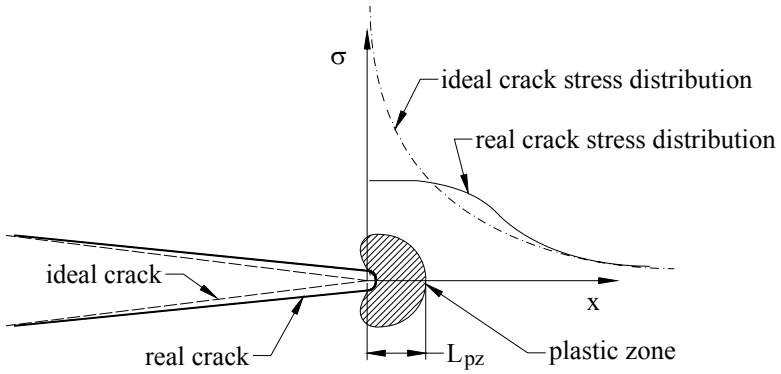

Figure 3.9: Finite stresses and region of plasticity at crack tip (non-linear fracture mechanics)

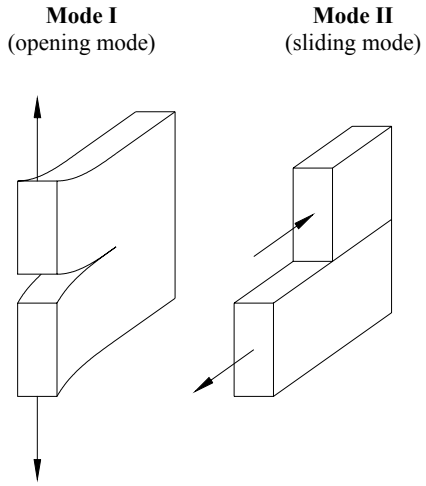

Figure 3.10: Two possible failure modes of wood described by fracture mechanics (after Jorissen, 1998)

Jorissen included shear stress analysis based on a model advanced earlier by Volkersen (1938). Jorissen assumed that the load P is completely transferred by the area between the two cracks, $2bt_u$ (Figure 3.12) and that the shear deformation is concentrated in a "fictitious layer".

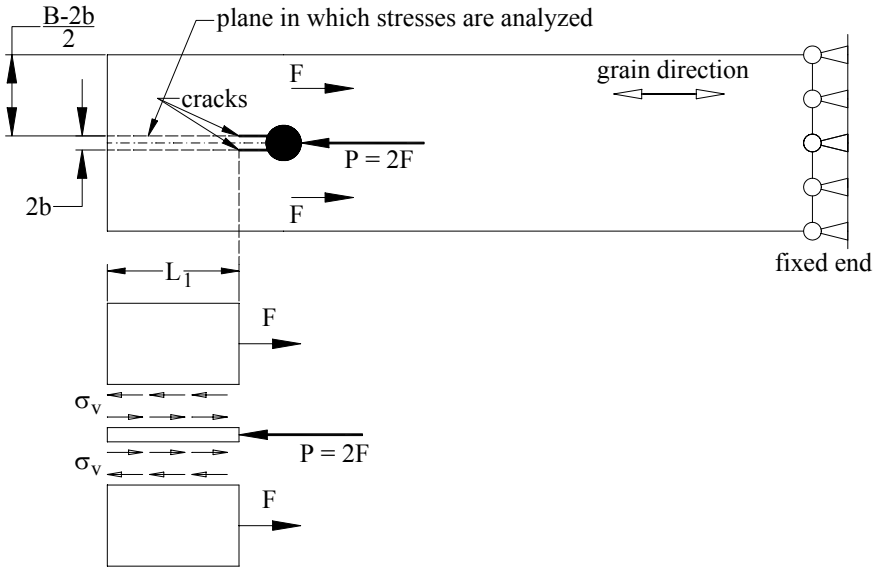

Figure 3.11: Shear stress as modeled by Jorissen (1998)

The stress function perpendicular to the grain (excluding peak stresses) was computed based on beam on elastic foundation theory, taking both bending and shear deflections into account. Assuming a linear elastic foundation, the foundation modulus for wood perpendicular to the grain, *k*, was approximated by

$$k = \frac{E_{90} \cdot t_u}{0.25 \cdot B} \tag{3.27}$$

and resulting stress distribution perpendicular to the grain as approximated by the model is depicted in Figure 3.12.

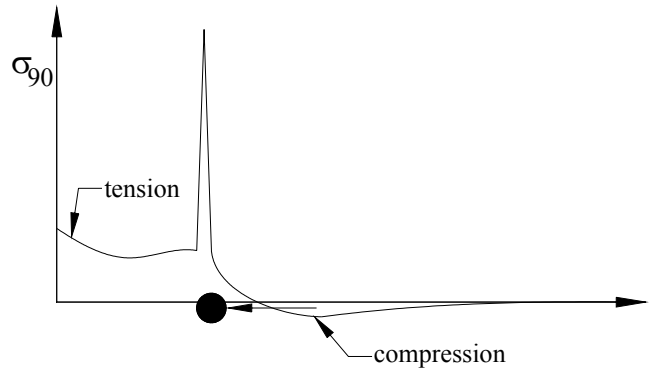

Figure 3.12: Stress distribution of stresses perpendicular to the grain including peak stresses (after Jorissen, 1998)

		Unit
t_u	fastener length with uniform embedment stress	mm
E_{90}	modulus of elasticity perpendicular to the grain	N/mm^2
k	foundation modulus	N/mm^2
B	member width	mm

Using the mechanical model shown in Figure 3.7, Jorissen determined the load per fastener. Subsequently, with the stress models discussed above, the accumulation of shear stresses and stresses perpendicular to the grain could be determined for each fastener location. However, as the computed stresses might exceed the maximum strength of wood, Jorissen developed a computer program that iteratively reduced and redistributed fastener load. Joint capacity was assumed to be reached if the computed joint load between two successive iteration steps did not vary more than 0.5 percent.

The model's prediction of the load-slip relation was relatively poor, but good agreement with experimental data was achieved as to prediction of capacity.

3.4 Concluding Remarks

The study of the unidirectional behavior of joints is actually a specialization of the general case, joints subjected to random input including reversed cyclic loading or displacement. Mathematical models that have been devised to predict monotonic behavior of dowel-type joints all exclude important information such as effects due to displacement or loading history and energy dissipation. Despite the appealing nature of monotonic loading or displacement input, it is

rare in real structures. Buildings are subjected to many varying loads including wind gusts from various directions, snow loads, occupancy loads, and where applicable, possible random earthquake loads. Attributed to its rheological and non-linear elastic plastic characteristics, wood exhibits "memory". In other words, a joint will behave differently if it was preloaded.

It is not hard to see then that general analytical models accounting for random input are of increased complexity when compared to their more specialized monotonic counterparts. While some monotonic derivations such as failure models may be applicable for cyclic loading, analytical models for the general case are entirely different in structure as the next Chapter reveals.